Exploring the quantum nature of the radial degree of freedom of a photon via Hong-Ou-Mandel interference

Ebrahim Karimi,[1,*] Daniel Giovannini,[2] Eliot Bolduc,[1] Nicolas Bent,[1] Filippo M. Miatto,[1] Miles J. Padgett,[2] and Robert W. Boyd[1,3]

[1]*Department of Physics, University of Ottawa, 150 Louis Pasteur, Ottawa, Ontario, K1N 6N5 Canada*

[2]*School of Physics and Astronomy, SUPA, University of Glasgow, Glasgow G12 8QQ, United Kingdom*

[3]*Institute of Optics, University of Rochester, Rochester, New York 14627, USA*

(Received 27 October 2013; published 23 January 2014)

In quantum information, quantum systems and their properties offer unprecedented opportunities. Being able to harness additional degrees of freedom adds power and flexibility to quantum algorithms and protocols. In this work, we demonstrate that the radial transverse mode of a single photon constitutes one such degree of freedom. We do so by showing that we can tune the two-photon interference, a quintessential quantum effect and the basic constituent of many quantum protocols, by manipulating its radial transverse modal profiles. Our work, in addition to allowing for greater versatility of existing protocols and significantly increasing the information channel capacity, can inspire novel quantum information tasks.

DOI: 10.1103/PhysRevA.89.013829 PACS number(s): 42.50.Tx, 03.67.Ac, 42.25.−p, 42.50.Ex

I. INTRODUCTION

Implementing quantum protocols and algorithms in high-dimensional spaces requires engineering the interaction of several particles [1]. A possible alternative, proposed in [2], is to exploit several degrees of freedom (DOF) of a single particle, instead. An example of this scheme takes place in quantum optics when multiple properties of a single photon are jointly addressed. In particular, in addition to polarization and energy, the transverse profile of a single photon supplies two unbounded Hilbert spaces [3], which in polar coordinates are labeled by discrete radial and orbital angular momentum (OAM) indices [4,5]. OAM has received immense interest, classically for its mechanical features [6] and in quantum information, where multidimensional Hilbert spaces play a crucial role [7]. In fact, OAM itself provides an unbounded Hilbert space, which can be used for implementing qudit states (the units of quantum information) [8]. In this way, encryption and decryption of information in a higher dimensional Hilbert space can be achieved with a lower number of photons, thus increasing the information density [9]. Moreover, OAM is robust against imperfections and noise during generation, detection, and transmission processes [10]. Combining polarization and OAM of photons, i.e., working with either polarization-OAM hybrid or hyperentangled states, has led to novel quantum communication schemes [11–13]. In a similar way, exploiting an additional, independent DOF (such as the radial mode) allows one to encode more qudit states in an individual photon. This independent infinite-dimensional Hilbert space might be combined with the others to further increase the capacity of a communication channel, the security of quantum key distribution protocols, and the processing speed in quantum algorithms.

Some of the properties of physical systems appear only at the classical level. For example, while one can use the optical phase to distinguish large enough coherent states, one cannot use it to differentiate single-photon states. In the same spirit, we aim at showing that radial modes can be successfully used to label distinct *single-photon* quantum states. This can be assessed in the quintessentially quantum context of Hong-Ou-Mandel (HOM) interference, where any property that can help distinguish the photons leads to a positive contribution to the probability of the photons leaving from different ports. HOM interference has been shown for DOF such as wavelength [14], polarization [15], Hermite-Gauss transverse modes [16], and OAM [17–19]. Consequently, several quantum gates and algorithms, e.g., the C-NOT gate and Shor's algorithm, and measuring parametric down-conversion spectra were proposed or demonstrated with some of those degrees of freedom [20,21]. Moreover, correlations in the radial mode of entangled photon pairs generated in down-conversion [22] have been explored in [23], raising the interest in the use of this DOF. The quantum nature of radial modes and OAM is quite different from that of the Cartesian modes, i.e., Hermite-Gauss modes [16], although both describe transverse modes of optical fields. In this article, we employed HOM interference to show experimentally that the radial DOF of single photons provides an additional unbounded discrete Hilbert space.

II. RADIAL INDEX OF LAGUERRE-GAUSS MODES

The transverse structure of any paraxial optical field, neglecting its vectorial characteristic (i.e., polarization), can be decomposed into the Laguerre-Gauss basis, whose eigenstates form a complete basis of transverse spatial modes in cylindrical coordinates. Laguerre-Gauss modes are labeled by two independent parameters: ℓ and p, which correspond to the azimuthal and radial quantum numbers, respectively, and can be compactly referred to as LG_p^ℓ [4]. As radial modes with the same value of ℓ are mutually orthogonal, and as there is in principle an infinite number of them, the corresponding Hilbert space is unbounded, but unlike OAM, the symmetry group associated with the radial DOF of an optical field is a noncompact SU(1,1) Lie group [5]. It has been theoretically proven and experimentally verified that considering the radial DOF of an entangled photon pair generated in nonlinear

*ekarimi@uottawa.ca

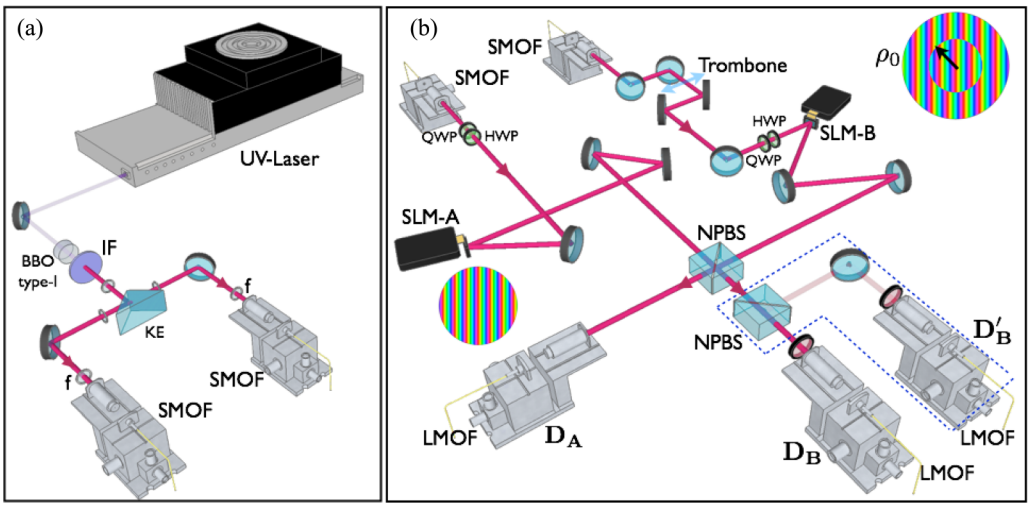

FIG. 1. (Color online) (a) Experimental setup for generating entangled photon pairs: The photon pair generated via spontaneous parametric down-conversion is made indistinguishable in all internal degrees of freedom by being coupled to single-mode optical fibers (SMOF), where only the Gaussian transverse mode is selected. They are then sent to the main apparatus, **b**, in order to demonstrate the HOM interference. (b) Experimental setup to test the Hong-Ou-Mandel interference: A quarter-wave (QWP) and half-wave (HWP) plates are used to compensate and rotate the polarization state of both signal and idler photons to horizontal (suitable to obtain a maximum efficiency at the spatial light modulators). Appropriate kinoforms are displayed on both spatial light modulators, SLM–A and SLM–B, to manipulate the radial DOF of the two photons and to render them completely indistinguishable, partially distinguishable or completely distinguishable. The insets near the SLMs show two possible types of holographic kinoforms. The two photons interfere on a 50:50 symmetric nonpolarizing beam splitter (NPBS). Then, they are collected by low-mode optical fibers (LMOF) coupled to single-photon counting modules (D_A and D_B), and detected in coincidence. In order to check the HOM coalescence enhancement, an additional NPBS is inserted in arm–B (blue dashed area), and the coincidence counts are read between detector D_B and D'_B.

down-conversion greatly increases the entanglement strength, and leads to an OAM/p-number hyperentangled state [23,24]. The difficulties associated with the study of radial modes include: (i) The chosen basis is beam-waist dependent; an eigenstate for a specific beam waist turns into a superposition of p modes for any other beam waist. (ii) The accurate generation of a specific LG_p^ℓ is challenging because it requires intensity masking with a phase-only hologram.

Hereafter, we assume only the radial profile of the optical beam as relevant, and that the other quantum numbers are identical. In particular, we take $\ell = 0$ in the rest of the paper. Therefore, the optical field modes are labeled only by the radial number p, i.e., $|\psi\rangle = \sum_{p=0}^{+\infty} c_p |p\rangle$, where $|p\rangle$ stands for a radial eigenmode of radial number p. The expansion coefficients c_p are normalized to one, i.e., $\sum_{p=0}^{\infty} |c_p|^2 = 1$. Since Laguerre-Gauss modes are mutually orthogonal, we have $\langle p|p'\rangle = \delta_{p,p'}$.

III. EXPERIMENTAL RESULTS

In our experiment, we prepared two photons, called signal and idler, in a down-conversion process. A frequency-tripled quasi-cw mode-locked Nd-YAG laser (repetition rate of 100 MHz, and average output power of 150 mW at 355 nm) pumped a 3-mm-thick nonlinear β-barium borate crystal cut for type-I phase matching in a near-collinear regime to generate identical photon pairs with degenerate frequency of $\lambda = 710$ nm. The generated photon pairs were coupled into two identical single-mode optical fibers where the TEM_{00} mode was selected, i.e., the transverse spatial mode of each photon was filtered by coupling into a single-mode optical fiber. Then, they were sent to the main apparatus in order to test the HOM coalescence. An overall quantum efficiency of 20% with a coincidence rate of 37 kHz was obtained by optimal splitting the photon pairs by a knife-edge (KE) prism; see Fig. 1(a). The polarization shift of signal and idler induced by the fiber propagation was compensated for by a combination of quarter-wave and half-wave plates, also used to set the polarization to horizontal in order to obtain the maximum efficiency of the spatial light modulators. At this stage the two photons are not anymore entangled, rather they are only synchronized in time. The radial modes of signal and idler, initially a Gaussian mode with waist of $w_0 = 954\,\mu$m, were controlled by two computer-generated holograms of 1920 $\times$ 1080 pixels displayed on two HOLOEYE PLUTO spatial light modulators (SLMs). The desired modes generated at the first order of diffraction of blazed kinoforms shown on the SLMs were then sent into a 50:50 symmetric nonpolarizing beam splitter (NPBS). The output beams were, then, coupled to low-mode optical fibers (LMOFs) with a core of 10 μm after being spectrally filtered by an interference filter (IF) with a bandwidth $\Delta\lambda = 10$ nm. During a fully automatic process, the photons were detected by two silicon module avalanche photodiodes, and finally a National Instrument data acquisition card recorded photon counts and coincidences between the signal and idler detectors with a detection window of 25 ns. A "trombone," an optical delayer, with a step size of $1\mu m$ was used to synchronize the arrival time of the photons on the NPBS.

We perform two tests of indistinguishability: measurement of the visibility of the standard HOM interference and what we termed "coalescence enhancement" (CE). CE is an additional

test that is performed to verify the interference effect. While two perfectly distinguishable photons do not coalesce at a balanced NPBS and one-fourth of the times leave the NPBS together from a specific port, in a configuration including the second beam splitter two indistinguishable photons leave the NPBS from the same port together half of the times. Therefore, the coincidence counts recorded by D_B and $D_{B'}$ after the photons pass through the second NPBS will double; see Fig. 1(b). In general, the enhancement $\mathcal{C}$ satisfies $1 \leqslant \mathcal{C} \leqslant 2$ and depends on the distinguishability of the photons. As a first step, two LMOFs were replaced with single-mode fibers and a standard HOM dip between two Gaussian photons was observed with a visibility of 0.987. Instead, due to a nonperfect post-selection by LMOFs, a visibility of 0.725 was achieved with the same setup. The visibility value was improved to 0.80 by setting up apertures at the far field of LMOFs, the SLMs position, to emphasise that the indistinguishability can be recovered by a fiber-independent spatial filtering. Nonetheless, the CE was very close to the theoretical value, since it provides an indistinguishability test that is less affected by experimental imperfections. Then an SLM manipulates the radial DOF such that signal and idler become effectively indistinguishable in all degrees of freedom except for the radial one, which we can adjust to be either (i) identical, (ii) partially different or (iii) entirely different; see Fig. 1 for details. As anticipated, the radial states of each of the two photons, in general, are $|\psi_s\rangle = \sum_{p=0}^{+\infty} c_p^s |p\rangle$ and $|\psi_i\rangle = \sum_{p=0}^{+\infty} c_p^i |p\rangle$, respectively, where c_p^s and c_p^i determine the distinguishability of the photons. The two states are indistinguishable if the overlap of the two satisfies $\langle\psi_s|\psi_i\rangle = 1$, and conversely are entirely distinguishable if $\langle\psi_s|\psi_i\rangle = 0$. A partial distinguishability is expected for a partial overlap between the two states. For instance, a state with only the $p = 0$ component (a Gaussian state) is orthogonal to any superposition that has no $p = 0$ component. This special case will be demonstrated in our experiment.

Generating a beam possessing specific radial momentum quanta with efficient phase-only SLMs requires intensity masking. The mask employs only a part of the SLM surface, so that it diffracts the required beam into the first order. However, the count rate decreases linearly with the extent of the surface undergoing intensity masking, thus affecting the coincidence count rate quadratically. In order to avoid such a technical difficulty, in the first part of the experiment we introduced a different type of holographic kinoform (phase-only computer generated holograms), where the whole SLM surface was used. Consequently, the coincidence rate was constant during all the experimental tests. Moreover, it allowed us to demonstrate the orthogonality among an infinite set of states in the radial Hilbert space. Our kinoform is made of a blazed grating with a centered disk of radius ρ_0 and of π phase shift with respect to the outer surface, as shown in the upper inset of Fig. 1(b). Diffraction of a Gaussian beam from such a kinoform at the first order is given by

$$\mathcal{E}(\rho) = \sqrt{\frac{2}{\pi}}\, e^{-\rho^2} \begin{cases} -1 & \rho < \rho_0 \\ +1 & \rho > \rho_0 \end{cases}, \tag{1}$$

where $\sqrt{2/\pi}$ is a normalization constant. The beam can be expanded in the LG basis with fixed ℓ, in this case $\ell = 0$: $\mathcal{E}(\rho) = \sum_{p=0}^{+\infty} c_p(\rho_0)\, \mathrm{LG}_p(\rho)$, where we omit the azimuthal index. The LG_p modes in the dimensionless coordinate at the pupil are

$$\mathrm{LG}_p(\rho) = \sqrt{\frac{2}{\pi}}\, e^{-\rho^2}\, L_p(2\rho^2), \tag{2}$$

where $L_p(.)$ are the Laguerre polynomials of order p. The expansion coefficients, then, can be calculated by $c_p(\rho_0) = 2\pi \int_0^{+\infty} \rho\, d\rho\, \mathrm{LG}^*{}_q\, p(\rho)\mathcal{E}(\rho)$ and are given by

$$c_p(\rho_0) = 4\rho_0^2\, {}_1F_1\left(p+1, 2, -2\rho_0^2\right) - \delta_{p,0}, \tag{3}$$

where ${}_1F_1$ and δ are a hypergeometric and Kronecker delta function, respectively.

The disk radius ρ_0 can be adjusted such that the Gaussian component of the diffracted beam is entirely suppressed, which happens at $\rho_0 \approx 0.588 w_0$. We rendered the photon

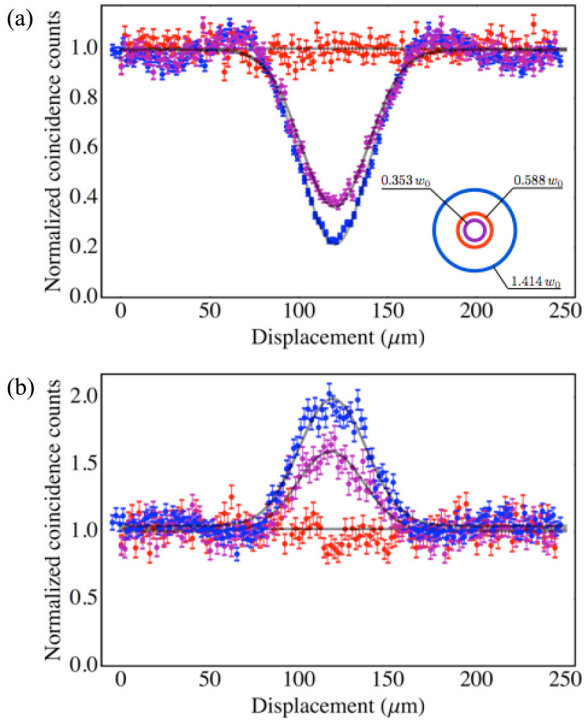

FIG. 2. (Color online) (a) Experimental data of the Hong-Ou-Mandel interference in the radial DOF (coincidence detection with D_A and D_B): The HOM dip indicates indistinguishability between the two photons; the flat data (red) corresponds to two completely distinguishable radial states, while the other two curves (magenta and blue) correspond to a pair of partially distinguishable and indistinguishable radial states. The visibilities of the dips are $\mathcal{V} = 0.014 \pm 0.027$, $\mathcal{V} = 0.465 \pm 0.030$, and $\mathcal{V} = 0.646 \pm 0.026$, respectively. The inset shows that the radius of each holographic kinoform displayed on the SLM-B which determined the value of the distinguishability. (b) Experimental data of the Hong-Ou-Mandel coalescence enhancement (coincidence detection with D_B and $D_{B'}$); the enhancement increases for indistinguishable photons in the radial DOF. The enhancements due to coalescence are $\mathcal{C} = 1.113 \pm 0.093$, $\mathcal{C} = 1.590 \pm 0.060$, and $\mathcal{C} = 1.907 \pm ,0.047$, respectively. The error bars correspond to one standard deviation and were calculated from a Poisson distribution. Solid curves are the best theoretical Gaussian fit. Note that the normalization factor for (a) and (b) are different.

TABLE I. Theoretical value of expansion coefficients (c_0), expected theoretical, and experimental observed HOM coalescence enhancements for various values of the circle radius ρ_0.

ρ_0	$\lvert c_0\rvert^2$	Theoretical $\mathcal{C}$	Experimental $\mathcal{C}$
0.000	1.000	$\mathcal{C} = 2.00$	$\mathcal{C} = 1.973 \pm 0.051$
0.353	0.310	$\mathcal{C} = 1.69$	$\mathcal{C} = 1.590 \pm 0.060$
0.588	0.000	$\mathcal{C} = 1.00$	$\mathcal{C} = 1.113 \pm 0.093$
1.414	0.928	$\mathcal{C} = 1.92$	$\mathcal{C} = 1.907 \pm 0.047$

pairs completely distinguishable by displaying a normal diffraction grating on SLM-A and a kinoform with a π phase jump at radius $\rho_0 \approx 0.588 w_0$ on SLM-B, as shown in Fig. 2(a) (red data points). In this situation, the photon pairs do not interfere, and the coincidence counts are effectively constant as a function of the trombone displacement, which yields a visibility of the HOM dip of $\mathcal{V} = 0.014 \pm 0.027$. Consequently, no CE [red points shown in Fig. 2(b)] was observed between detectors D_A and D_B, placed after the first beam splitter.

After having verified the ability of radial modes to effectively label quantum states, we increased the distinguishability of the photons by changing the radial position of the π jump on SLM-B to $\rho_0 = 0.353 w_0$ and $\rho_0 = 1.414 w_0$, and measured corresponding visibilities of $\mathcal{V} = 0.465 \pm 0.030$ and $\mathcal{V} = 0.646 \pm 0.026$, and CEs of $\mathcal{C} = 1.590 \pm 0.060$ and $\mathcal{C} = 1.907 \pm 0.047$ (see Fig. 2 for more details).

In Table I we show the expected theoretical and observed CEs and the first-order expansion coefficient c_0 for different values of circle radius.

We then observe the HOM interference between two identical spatial modes with no Gaussian component. A CE of $\mathcal{C} = 1.946$ was observed, which shows an excellent indistinguishability between two photons with identical superpositions of $p \geqslant 1$ modes. This last test is performed using a large portion of the Hilbert space of the radial DOF. Imperfections in the system, such as aberrations in the SLMs, alignment, and environmental issues prevented the minimum of the coincidence dip to reach exactly the value of zero. These effects are mostly noticeable by the necessary implementation of LMOFs.

In order to ensure that the radial DOF provides an additional unbounded discrete Hilbert space in addition to OAM, polarization, and wavelength, we examine the orthogonality between mutual radial states p_s and p_i. The recently developed *intensity-masking* technique is used to generate different radial eigenstates within a very good approximation [25]. The fidelity of generated state, however, is bounded by the pixel size, effectively employed active area of SLM, and the so-called SLM *gamma function* modulation. Nonetheless, an average fidelity about 0.98% for complicated transverse states is observed in prior work [26]. In this case, low-mode optical fibers at the detection stage (D_A and D_B) are replaced with 200-μm core-size multimode optical fibers, since low-mode optical fiber supports only few radial modes.

The experimentally observed visibility of the HOM dip for different radial eigenstates of $\{|0\rangle, \ldots |9\rangle\}$ is shown in Fig. 3. As seen in Fig. 3, two photons are perfectly

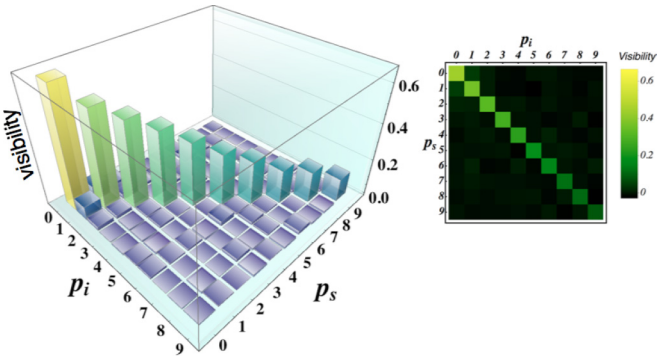

FIG. 3. (Color online) Experimental data of visibility of the HOM interference for two different radial modes of p_s (signal) and p_i (idler). The top right inset is a density plot of the three-dimensional plot. This shows that the eigenstates of the radial mode are mutually orthogonal; thus the associate Hilbert space is discrete and unbounded. Decreasing in visibility for higher p eigenstates is caused by truncation introduced by optics and a relatively small active area of the SLMs.

distinguishable when they possess different radial eigenstates. Due to experimental imperfection in which some of them discussed above the visibility for indistinguishable photons varies in the range of 32%–62%. Truncation, mainly introduced by microscope objectives and aperture of optics, and effective limited active area by SLMs are the main source of this imperfections in which alters the radial states. Thus, they reduce the visibility for higher values of p eigenstates. However, the presented data are good enough to show that the eigenstates of radial DOF are mutually orthogonal and unbounded.

IV. CONCLUSIONS

We have shown that the radial degree of freedom of *single photons* can be manipulated individually in a quantum regime and that it effectively acts as an additional label that allows us to adjust the distinguishability of two photons. This test was performed using quantum two-photon interference, the Hong-Ou-Mandel effect: We demonstrated that two photons with identical radial states coalesce, which is a consequence of their bosonic nature, and that they do not coalesce if their states are labeled by different orthogonal radial modes. It is our hope that the results and techniques presented here will inspire the ideation of novel quantum protocols and algorithms using the radial DOF in addition to the other degrees of freedom of light [18,20].

ACKNOWLEDGMENTS

The authors thank Jonathan Leach and Fabio Sciarrino for helpful discussions. E.K., E.B., N.B, F.M.M., and R.W.B. acknowledge the support of the Canada Excellence Research Chairs (CERC) Program. D.G. acknowledges the support of the EPSRC. E.B. acknowledges the financial support of the FQRNT, Grant No. 149713. M.J.P. thanks the EPSRC and the Royal Society. R.W.B. and M.J.P. were also supported by the DARPA InPho program.

[1] E. Knill, R. Laflamme, and G. J. Milburn, Nature (London) **409**, 46 (2001).
[2] D. Salart, O. Landry, N. Sangouard, N. Gisin, H. Herrmann, B. Sanguinetti, C. Simon, W. Sohler, R. T. Thew, A. Thomas, and H. Zbinden, Phys. Rev. Lett. **104**, 180504 (2010).
[3] L. C. Dávila Romero, D. L. Andrews, and M. Babiker, J. Opt. B: Quantum Semiclass. Opt. **4**, S66 (2002).
[4] L. Allen, S. M. Barnett, and M. J. Padgett, *Optical Angular Momentum* (Institute of Physics, Bristol, 2003).
[5] E. Karimi, and E. Santamato, Opt. Lett. **37**, 2484 (2012).
[6] N. B. Simpson, L. Allen, K. Dholakia, and M. J. Padgett, Opt. Lett. **22**, 52 (1997).
[7] S. Franke-Arnold, L. Allen, and M. J. Padgett, Laser Photon. **2**, 299 (2008).
[8] G. Molina-Terriza, J. P. Torres, and L. Torner, Nat. Phys. **3**, 305 (2007).
[9] J. Leach, E. Bolduc, D. J. Gauthier, and R. W. Boyd, Phys. Rev. A **85**, 060304 (2012).
[10] D. Giovannini, E. Nagali, L. Marrucci, and F. Sciarrino, Phys. Rev. A **83**, 042338 (2011).
[11] J. T. Barreiro, N. K. Langford, N. A. Peters, and P. G. Kwiat, Phys. Rev. Lett. **95**, 260501 (2005).
[12] V. D'Ambrosio, E. Nagali, S. P. Walborn, L. Aolita, S. Slussarenko, L. Marrucci, and F. Sciarrino, Nat. Commun. **3**, 961 (2012).
[13] J. T. Barreiro, T. C. Wei, and P. G. Kwiat, Nat. Phys. **4**, 282 (2008).
[14] C. K. Hong, Z. Y. Ou, and L. Mandel, Phys. Rev. Lett. **59**, 2044 (1987).
[15] M. H. Rubin, D. N. Klyshko, Y. H. Shih, and A. V. Sergienko, Phys. Rev. A **50**, 5122 (1994).
[16] S. P. Walborn, A. N. de Oliveira, S. Pádua, and C. H. Monken, Phys. Rev. Lett. **90**, 143601 (2003).
[17] E. Nagali, F. Sciarrino, F. De Martini, L. Marrucci, B. Piccirillo, E. Karimi, and E. Santamato, Phys. Rev. Lett. **103**, 013601 (2009).
[18] E. Nagali, L. Sansoni, F. Sciarrino, F. De Martini, L. Marrucci, B. Piccirillo, E. Karimi, and E. Santamato, Nature Photo. **3**, 720 (2009).
[19] E. Nagali, D. Giovannini, L. Marrucci, S. Slussarenko, E. Santamato, and F. Sciarrino, Phys. Rev. Lett. **105**, 073602 (2010).
[20] P. Kok, W. J. Munro, K. Nemoto, T. C. Ralph, J. P. Dowling, and G. J. Milburn, Rev. Mod. Phys. **79**, 135 (2007).
[21] H. Di Lorenzo Pires, H. C. B. Florijn, and M. P. van Exter, Phys. Rev. Lett. **104**, 020505 (2010).
[22] F. M. Miatto, A. M. Yao, and S. M. Barnett, Phys. Rev. A **83**, 033816 (2011).
[23] V. D. Salakhutdinov, E. R. Eliel, and W. Löffler, Phys. Rev. Lett. **108**, 173604 (2012).
[24] F. M. Miatto, H. Di Lorenzo Pires, S. M. Barnett, and M. P. van Exter, Eur. Phys. Journal D **66**, 1 (2012).
[25] E. Bolduc, N. Bent, E. Santamato, E. Karimi, and R. W. Boyd, Opt. Lett. **38**, 3546 (2013).
[26] V. D'Ambrosio, F. Cardano, E. Karimi, E. Nagali, E. Santamato, L. Marrucci, and F. Sciarrino, Sci. Rep. **3**, 2726 (2013).